

International Conference on Space Optics—ICSO 2006

Noordwijk, Netherlands

27–30 June 2006

Edited by Errico Armandillo, Josiane Costeraste, and Nikos Karafolas



Design and performance of the lightning imager for the Meteosat third generation

*Leonardo Tommasi, Giuseppe Basile, Andrea Romoli,
Moreno Stagi*



DESIGN AND PERFORMANCE OF THE LIGHTNING IMAGER FOR THE METEOSAT THIRD GENERATION

Leonardo Tommasi, Giuseppe Basile, Andrea Romoli, Moreno Stagi

Galileo Avionica, Via A. Einstein 35 - 50013 Campi Bisenzio - Italy, Email: leonardo.tommasi@galileoavionica.it

ABSTRACT

In the frame of the MTG Pre-Phase A study, feasibility of an instrument to fulfill the goals of the Lightning Imagery Mission has been investigated. Architecture is based on a set of four optical heads, each dedicated to observation of a fraction of the Earth disk and including a telescope, a narrow band filter, a detector and its proximity electronics. In particular, detector is characterized by a novel pixel architecture that provides autonomous lightning identification and readout of the flash data with a very high rate, reducing throughput at a minimum. This allows the instrument to fulfill mission objectives in terms of spatial and temporal resolution, with the lowest mass and power allocation. Details on instrument concept, design and budgets, as well as performance evaluation for different operative scenarios (day/night) are provided.

1. INTRODUCTION

According to latest issue of [1], a Lightning Imagery mission is foreseen as part of the Meteosat Third Generation (MTG) mission. Its primary objective is to add complimentary information to the existing ground lightning detection systems, with the benefit to provide a much wider coverage, including poorly populated areas, and a reference to correlate different ground systems and networks. Additional objectives of the mission are contribution to climate and atmospheric chemistry monitoring through observation of distribution and long term effects of lightning.

Mission is required to provide continuous coverage of specified FOV, with measurement of each flash location epoch and energy content. Real time processing and data distribution within 20 s are expected. Other mission requirements as contained in [1] are reported in Tab. 1.

Note that after initial discussion of the impact of each requirement on instrument design, a lower detection probability for the minimum energy flash (about 50%) has been agreed with the Agency, to avoid very large optical aperture.

Starting from the outcome of the previous Post-MSG studies in [2] and [3], an instrument design fulfilling the requirements of Lightning Imagery mission has been elaborated during MTG pre-phase A study, as

described in section 2 here below. In the following section 3, Lightning Imager (LI) performance are illustrated under different operative scenarios. Finally, some conclusions are given in section 4.

Tab. 1. Lightning Imagery Mission requirements.

Requirement	Value	Notes
Wavelength	777.4 nm	0.34 nm bandwidth
Coverage	16°	
IFOV	10 km	@ 45° latitude
Sensitivity	90%	4.0 $\mu\text{J}/\text{m}^2/\text{sr}$
False alarms	$< 1 \text{ s}^{-1}$	Over full FOV
Dynamic range	100	4 to 400 $\mu\text{J}/\text{m}^2/\text{sr}$
Radiometric accuracy	$< 50\%$	20% goal

2. LIGHTNING IMAGER DESIGN

Lightning Imager design has been elaborated to achieve best compliance with mission requirements (Tab. 1) with the minimum use of spacecraft resources. Design is based on the adoption of four optical heads, each one observing a quadrant of the total requested FOV and including a baffle, telescope, detector and proximity electronics. This choice has a twofold impact on instrument design. First, number of pixels needed to achieve the desired IFOV on each detector is reduced to one fourth (with lowered readout frequency and detector size). Secondly, narrower spectral band width is possible, with significant impact on instrument SNR.

Lightning Imager instrument is constituted by the following elements:

- 4 optical heads, each including:
 - Baffle
 - Telescope
 - Focal Plane Assembly (FPA)
 - Proximity Electronics (PE)
- 1 Main Electronics (ME)

2.1 Optics

Each of the four telescopes has been designed to meet the radiometric (aperture) and geometric (IFOV and FOV) requirements with a 40 μm pitch detector. A summary of the optical system is contained in Tab. 2.

Tab. 2. Optics summary specification.

Parameter	Value
Pupil diameter	160 mm
Optics transmission	90%
Focal length	200 mm
FOV	8° x 8°
Filter band pass	1.4 nm
Filter transmission	60%

Optics design has been oriented to the simplest solution in terms of number and feasibility of optical elements, in full compliance with radiation hardness requirements of the space environment. Result is a catoptric layout constituted by four lenses, with only one aspheric surface (first of the first element), as illustrated in the Fig. 1. Selected material is fused silica for all the lenses but the second one, that is manufactured in ZnS.

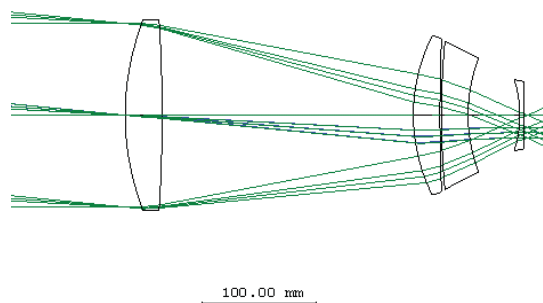


Fig. 1. Optical layout (each telescope).

In addition to filter specification reported in Tab. 2 (transmission and bandwidth) it shall be observed that a filter minimum diameter equal to the useful telescope aperture is needed for each telescope. This comes from the choice to place filter in front of the first lens of the telescope, any other position within the optical path resulting in a smaller diameter, but larger beam aperture, requiring a wider transmission bandwidth. This would reduce SNR due to less efficient background rejection. Notice that active control of filter temperature is foreseen, to avoid drift of the filter central wavelength during operations, with subsequent decreasing in SNR due to mismatch between flash spectral features and instrument band width.

Realisation of a filter with this specification is far from being straightforward. In particular, large diameter with a narrow bandwidth represents a challenging task since high coating uniformity has to be obtained over a large area. However, since filter specification are similar to that of other devices realised for space application (LMS GOES as from [4]), we can conclude that filter realisation does not represent a major technological issue.

A baffle has been designed to be placed in front of each telescope unit to reduce straylight from out of field sources. Baffle is characterised by its length, that can be basically related to the width of acceptance cone as in Fig. 2 (off axis angle refers to cone semi-aperture).

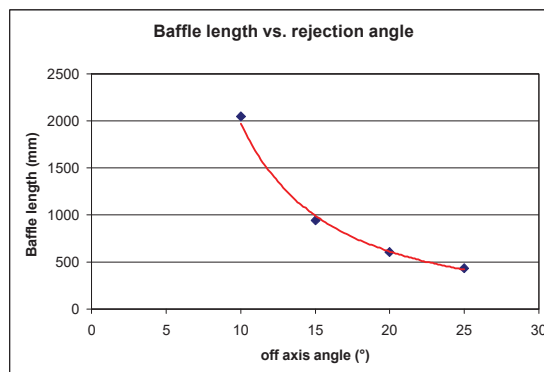


Fig. 2. Baffle length vs. rejection cone width.

An acceptance angle of 20° semi-aperture has been selected as a trade off, resulting in a 550 mm long baffle.

2.2 Detector and electronics

In the simplest possible data processing approach, one can imagine that all data collected by the Lightning Imager (LI) are digitised and acquired (4 detectors with 778 x 778 pixel each, simultaneously read every 0.8 ms), the throughput being as high as 36 Gbps. Detector can be a standard hybrid CMOS array, where all tasks of lightning information identification and extraction are in charge to the electronics. This can be still manageable through a large number of outputs from each detector and very fast electronics, but major drawback of a large complexity, power and mass arise. On the other hand, since only few pixels contain useful lightning information, the others only being a measure of the background (sun and moon irradiance, anthropic lights), a key to dramatically reduce throughput is to process the analogue signal as soon after integration, then acquire only those pixels that are found to have recorded a flash. Most effective way to reject background pixels is to evaluate background level on each pixel (by averaging a suitable number of frames) and to apply a threshold, adjusted to meet the given false alarm probability and detection efficiency. With a “smart” customised CMOS detector with an amount of analogue electronics integrated at pixel level this tasks can be performed on chip, so that only those pixels exceeding threshold are digitised and acquired. Data processing algorithm is illustrated in Fig. 3, where the two approaches described above are compared.

Electronics to be implemented on each pixel of the “smart” APS to determine background level and apply threshold is outlined in the following Fig. 4.

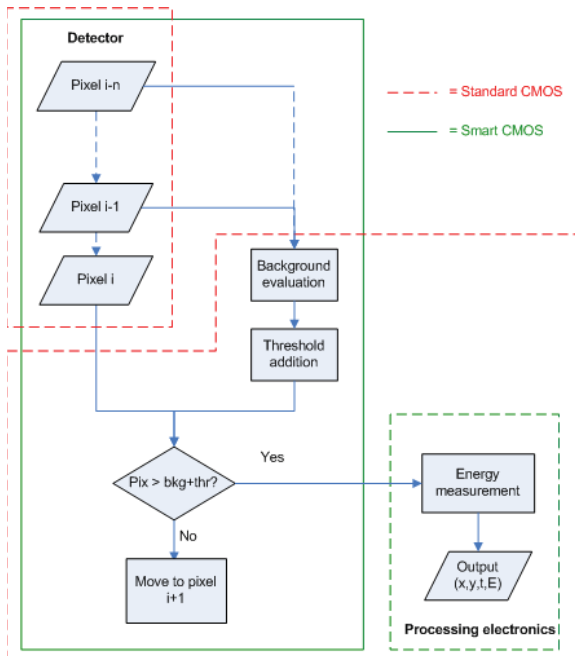


Fig. 3. Data processing algorithm and possible implementations.

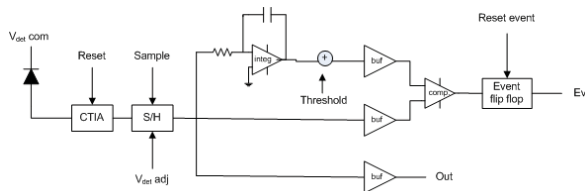


Fig. 4. “Smart” APS pixel architecture.

In addition to signal analogue output (Out), each pixel has a logic event output (Ev), whose value is high if that pixel level is found to exceed given threshold. All event outputs in a row are OR’ed together, resulting in a row event output (OR Rn event), that is high if one or more pixels in that row exceed threshold level.

Detector readout begins with a fast scan of the row events until one is found to be high, then that row is selected and pixel events and outputs are transferred to the output register. Then, complete scanning of the row is performed through sequential column addressing, starting conversion only when the pixel event is found high. Detector architecture to perform such a readout is illustrated in the Fig. 5.

Note that all readout electronics resides on chip, the only task of the proximity electronics being to generate biases and clocks for detector driving (in addition to data acquisition and HK readout). Moreover, a 12 bit

ADC can be cost-effectively implemented on chip. If desired, it can be electrically disconnected by the analogue output (e.g. analogue output and ADC input connected to distinct but adjacent pins), so making possible to switch to an external ADC, if appropriate, even after detector realisation.

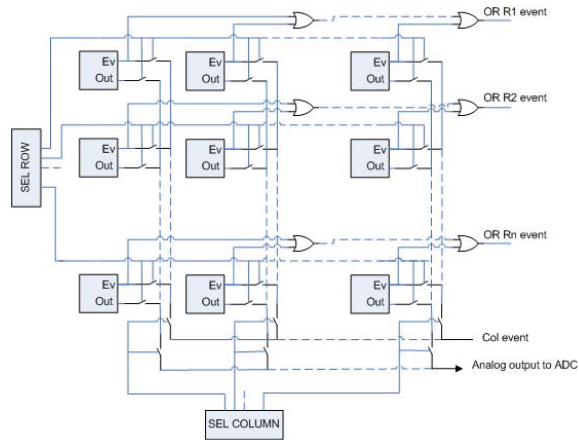


Fig. 5. “Smart” APS detector architecture.

To simplify detector layout, threshold level (to be added to the pixel-per-pixel estimated background) is assumed to be the same for all pixels. Moreover, although threshold level can be externally adjusted (e.g. after in flight calibration is performed), it is independent from the background level. This means that detection probability for a given flash energy is held constant, while false alarm rate varies accordingly to background radiance. Another approach is possible (in principle) in which threshold level is calculated according to the background variance, resulting in a constant false alarm rate, but a variable detection probability. This requires additional electronics to be implemented at a pixel or detector level if threshold calculation is desired for each pixel or for all pixels, respectively. However, its complexity shall be validated to assess feasibility.

Since the proposed readout approach is faster as lower is the number of detected flashes, an upper limit has to be placed to that number to maintain a constant 0.8 ms frame rate, including processing. It has been assumed that a maximum of 50 detected events per frame can be managed by the detector. This is considered sufficient to account for occurrence of several lightning within one integration time (temporal lightning clustering), as well as of spurious events, such as cosmic rays or detector defects (including ageing). Notice that on average about 1 lightning/ms is expected over the whole earth disk as from [5]. Should detector readout “saturate” due to a larger number of detected flashes, only the first 50 are correctly processed (without any loss of data), then a warning message is returned by the proximity electronics and processing of the next acquired frame begins. Assuming a maximum number

of 50 detected events per frame, the longest readout time occurs if events are distributed over 50 different rows. In this case, acquisition is completed through full scanning of 50 rows (identified by the state of their OR Row event outputs) with 778 pixels, and ADC conversion of the 50 events. Readout of the detector can be achieved within 0.8 ms (baseline integration time) provided that 50 MHz scanning and 1 Msps A/D conversion are adopted.

Feasibility of the “smart” architecture described above has been preliminarily assessed with a major European manufacturer (both pixel electronics and detector readout architecture) and, despite the high level of customisation required, such a detector appears feasible matching the mission requirements. So, this detector architecture has been retained as a baseline for the present instrument design, compatible with present status of European technology and currently on-going developments. Development time for the LI detector can be envisaged in two years.

A back illuminated monolithic APS is retained as a backup solution, with more solid heritage and shorter development time, with the drawback of a lower quantum efficiency. Specification of the two possible detectors are summarised in Tab. 3.

Tab. 3. Lightning Imager detector specification (baseline and backup option).

Parameter	Hybrid CMOS	Back illuminated APS
Quantum efficiency x fill factor	80 %	70 %
Well capacity to meet dynamics	$2 \times 10^6 e^-$	$1.5 \times 10^6 e^-$
Readout + fixed noise	$350 e^-$	$400 e^-$
Array format	778 x 778 pixels	
Pixel pitch	40 μm	
Operation	snapshot	
Frame rate	1000 fps	
Pixel detection	CTIA	
Max handling capacity	50 events/frame	
ADC	12 bit	

2.3 Instrument layout

The 4 optical heads shall be integrated on a single mechanical structure to assure co-alignment and stability between the four optical axis. A possible implementation of this element is represented in Fig. 6 and Fig. 7, where tentative support structure is outlined (3 thin supports for each telescope and baffle) and instrument size is specified (approximate, in millimeters).

In addition, ME box is present, whose size is $190 \times 263 \times 325 \text{ mm}^3$, including DC/DC and filter thermal control power. Entire ME is duplicated for redundancy, in order to meet the required lifetime.

Moreover, separate operation of each optical head is achieved. In this way, failure of an optical head involves loss of a fraction of the FOV, without representing a single point failure for the instrument.

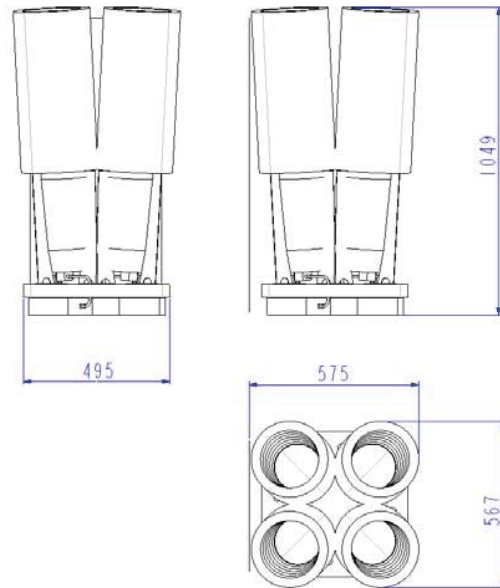


Fig. 6. LI size (excluding Main Electronics).

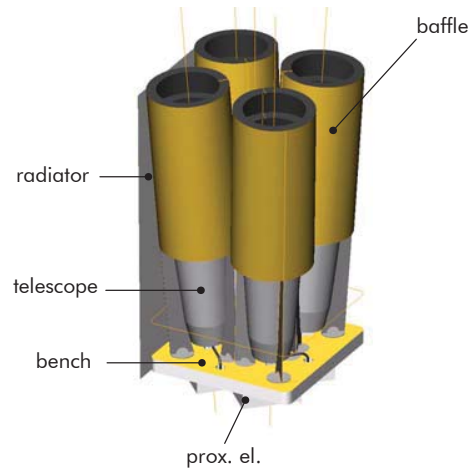


Fig. 7. View of present LI layout.

While Proximity Electronics is placed in the close vicinity of the detectors to reduce cable length at a minimum (back side of the bench), placement of Main Electronics box is not particularly critical. It can be accommodated either on the optical heads supporting structure bench or within S/C.

The assembly bench will be connected to the S/C platform by isostatic mounts in order to maintain a good isolation from stress/alignment point of view.

These items have been included in the mass budget, even if not shown in the previous Figures.

2.4 Budgets

In the following Tab. 4, LI mass budget is reported, where 20% contingency (compatible with present design status) is already included in the figures.

Tab. 4. Lightning Imager mass budget.

Element	Mass kg (incl. cont.)	Notes
Optical head (each) ¹	12.2	4 units
Radiator	3.6	
Bench (incl. S/C interface)	4.6	
Main Electronics ²	10.2	
Harness	4.8	
Lightning Imager	72.2	

¹ Includes filter, telescope, baffle, detector and proximity electronics

² Includes DC/DC and filter thermal power. Entire ME cold redundant included.

Power budget of the lightning imager is outlined in Tab. 5. Again, 20% contingency has been included.

Tab. 5. Lightning Imager power budget.

Element	Power W (incl. cont.)	Notes
Proximity Electronics	2.4	4 units
Main Electronics	70.8	
Lightning Imager	115 ¹	@ 28V

¹ 70% DC/DC efficiency assumed.

Amount of data for each event is calculated as in Tab. 6, assuming 16 bit words.

Tab. 6. Lightning Imager data volume (each flash).

Information	Data	Notes
Event X coord	1 word	
Event Y coord	1 word	
Event energy	1 word	
Date tag	1 word	Days elapsed since January 1 st 2000
Frame tag	2 words	0.8 ms/frame, resets every 24 hours
Checksum	1 word	

Assuming 2 pixels/flash on average (most flashes will be split over adjacent pixels) and 1000 flashes/s over the full FOV (8°x8°), average science data rate is 224 kbps.

No bad pixel has been included in the data rate budget, since threshold algorithm shall be able to automatically reject (by raising threshold level) those pixels that show a systematically high signal due to defects (including radiation induced) or non uniformity of dark signal and offset.

3. PERFORMANCE EVALUATION

LI performance are summarized in Fig. 8 and Fig. 9 for the baseline and backup detectors, respectively. Detection efficiency is plotted versus flash energy, for two different values of false alarm rate (number of false detections over the whole covered FOV). Worst case for flash detection (i.e. maximum background during day) is considered in both Figures.

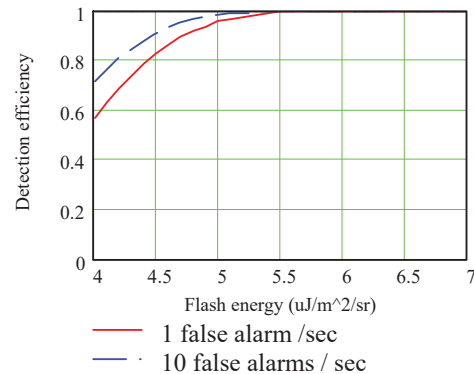


Fig. 8. Lightning Imager detection efficiency (baseline hybrid CMOS detector).

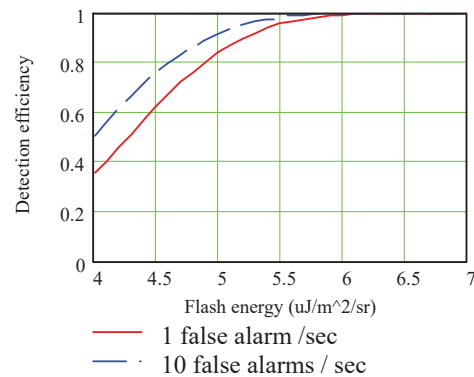


Fig. 9. Lightning Imager detection efficiency (backup monolithic back illuminated APS detector).

Finally, LI performance as a function of Sun Zenith angle are reported in Fig. 10, assuming baseline hybrid CMOS detector option. Plot shows flash energy for which 90% detection probability is achieved. Left and right ends of the curve represent worst daylight case (noon) and worst night time case (full Moon at zenith assumed), respectively. It can be observed that the original requirement (4 $\mu\text{J}/\text{m}^2/\text{sr}$ as in Tab. 1) is still fulfilled even during the day provided that Sun is $\sim 45^\circ$ or more apart from the Zenith. This condition is always verified for all central/northern Europe, minor exceptions occurring around Summer solstice at lower European latitudes.

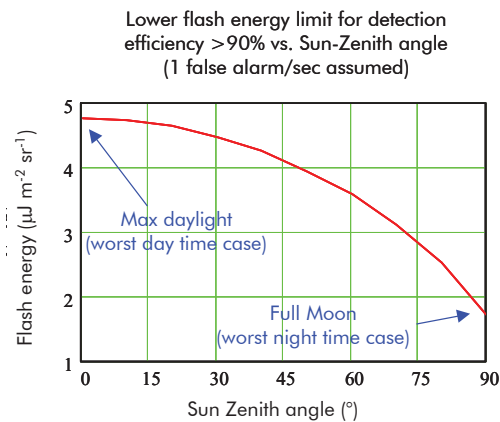


Fig. 10. LI minimum detectable energy (at 90% detection probability) vs. Sun-Zenith angle.

4. CONCLUSIONS

An optical payload instrument concept for the Meteosat Third Generation, compliant with the requirements of the Lightning Imagery mission have been elaborated during a pre-phase A mission study.

Instrument design has been performed basing on four optical heads with narrow band filters for solar background rejection, and customised detectors capable of on-chip data processing for flash identification. This is achieved by integrated electronics performing background determination and thresholding at each pixel level.

Feasibility of the most critical elements, namely the filter and the detector has been preliminarily assessed through contacts with major manufacturers.

A mathematical model has been prepared and used to evaluate instrument performance under different operative scenarios, showing that instrument is compliant with relevant mission requirements.

5. ACKNOWLEDGEMENTS

The Lightning Imager development described herein has been carried on under ESA contract in the frame of the MTG Pre-Phase A study led by Alcatel Alenia Space.

6. REFERENCES

1. Mission Assumptions and Technical Requirements Document for the MTG Mission pre-phase A System Study, EOP-FP/2003-03-771, Issue 1.1, October 2004
2. Post-MSG Observation Technique and Sensor Concept study, Final Report (Alcatel Space), PMSG-ASP-RP-30, Issue 1, 26/03/04

3. Post-MSG Observation Techniques and Sensor Concepts study, Final Report (Astrium SAS), EF.RP.FP.04.00093, Issue 1, 26/03/04
4. Manlief S.K. The lightning mapper sensor for GOES/NEXT, *proc. of the Space Programs and Technologies Conference*, Huntsville, 1992
5. Christian H.J. et al. The detection of Lightning from geostationary orbit, *J. Geophysical Research*, Vol. 94, 13329-13337, 1989